J MATER RES TECHNOL. 2020;9(4):7529–7539

Available online at www.sciencedirect.com

jmr&t Journal of Materials Research and Technology

www.jmrt.com.br

Original Article

Electrochemical study and gravimetric behaviour of gray cast iron in varying concentrations of blends as alternative material for gears in ethanol environment

Enesi Y. Salawu[a,*], Oluseyi O. Ajayi[a,c], Anthony O. Inegbenebor[a], Stephen Akinlabi[a,b,d], A.P.I. Popoola[c], Esther Akinlabi[a,b], Olugbenga A. Omotosho[a], U.O. Uyo[c]

[a] Department of Mechanical Engineering, Covenant University, Ota, Nigeria
[b] Department of Mechanical Engineering Science, University of Johannesburg, South Africa
[c] Department of Chemical, Metallurgical and Materials Engineering, Tshwane University of Technology, Pretoria, South Africa
[d] Department of Mechanical Engineering, Walter Sisulu University, South Africa

ARTICLE INFO

Article history:
Received 31 March 2020
Accepted 14 May 2020
Available online 5 June 2020

Keywords:
Spur gears
Corrosion
Failure
Cast iron

ABSTRACT

The phenomenon of chemical degradation of mild steel materials under ethanol environment is becoming alarming. In order to study the electrochemical, thermal and mechanical behaviour of gray cast iron in this environment, this paper deals with the investigation of gray cast iron sample in varying concentrations of different ethanol blend solution. The electrochemical behaviour of gray cast iron sample was studied in ethanol concentrations of A – 42%, B – 40%, C – 28%, D – 43% and E – 45% using distilled water as control medium. Observations of the microstructures after the test showed that mainly oxides and corrosion products dominate the surfaces. However, some areas showed some cracks which are less severe. Also, the thermal gravimetric analyses of samples after the electrochemical test showed that, there was reduced thermal decomposition which suggests its good performance for gear application. Further to this, the micro-hardness results showed that the material maintained its mechanical properties despite the interactions with the solvents.

1. Introduction

Production and packaging of blended ethanol beverages has many consequences on engineering materials especially bottle packaging plants at large due to the presence of chemical additives and consistent flow of water during sterilisation process. Cavitation erosion and micro pitting have been found to be the major failures associated with certain engineering components such as pump impeller and gears [1]. Ethanol as a solvent contains a hydroxyl group which have the ability to dissolve ionic compounds [2]. For instance, Tomić et al. [3], noted that chloride ion is present in ethanol blended with gasoline which can cause some uncertainties as a bio-based fuel. The chloride ions have the ability to penetrate through the surface asperities to the oxide films on mild steel, adsorbed on the surface of the metal and destroy the

* Corresponding author.
E-mail: enesi.salawu@covenantuniversity.edu.ng (E.Y. Salawu).
https://doi.org/10.1016/j.jmrt.2020.05.049

protective surface of the mild steel paving way for eventual corrosion [4]. Corrosion of steel has been a serious challenge to many researchers and scientist because of the low corrosion resistance especially in ethanol and water environment. For instance, droplets of this fluid on steel form a shock wave and attack the surfaces of components made from steel [5]. Consequently, the component being subjected to repeated rotation at high speed fails due to fatigue which eventually affects the overall productivity and machine reliability [6–8]. Indicating that, the certain additives in ethanol beverage can change the dynamics of material constituents, which introduced some unintended consequences in the machine components. Corrosion of mild steel in ethanol, water and acid is known to have posed huge loss to the industries as well as the society at large [9]. Although, many attempts have been made through various research involving the use of corrosion inhibitors. But, several hazard associated with chemical inhibitors have made researchers to focus on alternative material which can function in a corrosive environment [10–12]. Implying that the use of inhibitors for protection of metals is still a problem for material scientists. Based on these highlighted problems associated with mild steel, the issue of mild steel corrosion in ethanol and water environment can be addressed using alternative materials (like the gray cast iron) for developing components which can function in such aggressive environment. Gray cast iron is widely used in engineering applications owing to its, damping ability and lower cost [13]. It is one of the alloys with excellent tribological properties and it is suitable for gear applications [14]. Neville et al. [15], noted that the interactions between engineering components and electrochemical processes causes loss in weight which eventually affect the component performance in such environment. More so, the weight loss depends on the time of exposure, mass transfer and volume concentration of the environment [16]. Despite the problems associated with corrosion of metals, gray cast iron still finds applications in some environment. For instance, Al-Shama et al. [17], reported that cast iron survive in acidic environment due to the presence of certain inhibitor. Also, studies have revealed that certain modifications of gray cast iron helps in improving the mechanical properties of the material. For instance, chromium, nickel and molybdenum addition to gray cast iron resulted into a modification of the surface making it hard for subsequent applications [18–20]. Thus, these improved properties in gray cast iron deem it fit for use in certain aggressive environment. For instance, heat treated nodular cast iron showed better corrosion resistance and improved wear properties when subjected to sodium hydroxide solution [21]. Therefore, to address the challenges of long term and efficient performance of gear components, gray cast iron is preferable because of its better corrosion properties, resistance to deformation, resistance to oxidation and high compressive and tensile strength. Thus, gray cast iron is a promising alternative materials to be used in gears and other engineering components that can function in aggressive environment. This work therefore, focus on investigating the effects of electrochemical processes on the microstructural and the thermal gravimetric properties of coupons of gray cast iron subjected to varying concentrations of ethanol beverage blend solutions. Hence, a new approach desirable in mitigating the pitting corrosion in spur gears made from mild steel.

Table 1 – Chemical composition of gray cast iron.

C	Si	Mn	S	P	Fe
2.68	1.42	0.63	0.13	0.28	94.86

2. Experimental details

2.1. *Preparation of the substrate (gray cast iron)*

The studied gray cast iron is of grade HT250 with chemical composition as displayed in Table 1 with dimension 30 mm × 30 mm × 10 mm). Substrates were mounted to protect the edges from destruction during grinding and polishing. Additionally, polishing was done using different grades of SiC abrasives to remove the surface oxides and finally cleaned in 4% mixture of alcohol and nitric acid (nital) at room temperature for the purpose of etching the substrate to reveal the matrix of the microstructure. Fig. 1a showed the microstructure of the as received gray cast iron, while Fig. 1b showed the optical micrograph of the substrate after etching in nital. Both (Fig. 1a and b) showed flake graphite and pearlite which is an indication of white cast iron properties [22].

2.2. *Electrochemical measurement*

The corrosion rate measurement of the gray cast iron sample in varying concentrations of different ethanol blend was evaluated by potentiodynamic test. The corrosion test of gray cast iron sample in different blend of the ethanol solution was carried out at room temperature of 27 °C [13] with each sample in 50 mL of the ethanol blend at varying pH as shown in Table 2. The reference electrode was immersed into the solution for 60 min to achieve the stability of cyclic potentiodynamic polarisation test while tafel extrapolation and linear polarisation were measured at a scan rate of 0.005 v/s. In this test, data were obtained and recorded using autolab controlled potentiostat integrated with software (Nova 2.1.2) of built version 6333.

2.3. *Determination of polarisation resistance*

The polarisation resistance was determined using the basics of corrosion measurements adopted from Princeton Applied Research. The principle was applied to measure the absolute corrosion rate of each medium (polarisation resistance): the principle is:

$$\Delta E/\Delta t = \frac{\beta_A \beta_C}{2.3(I_{corr})(\beta_a + \beta_c)}$$

where; $\Delta E/\Delta i$ = slope of the polarisation resistance plot, ΔE is expressed in volts and Δi is expressed in μA. The slope has units of resistance, hence, polarisation resistance. $\beta_A\beta_C$ = anodic and cathodic Tafel constants (which were determined from a Tafel analysis in the Nova 2.1.2 software.

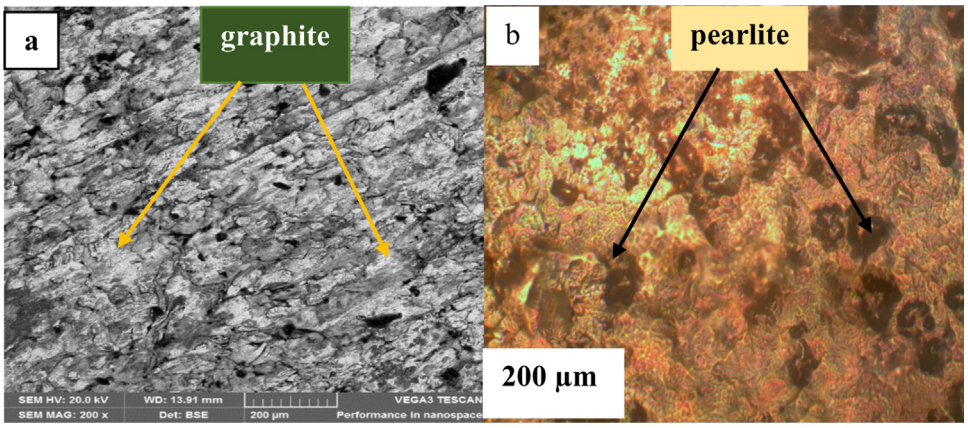

Fig. 1 – (a) SEM morphology of as received gray cast iron (b) Optical micrograph after etching the as-received gray cast iron in 4% natal.

Table 2 – Properties of Ethanol blend solution.

S/N	Sample ID	% Conc.	pH	Conductivity (µs/cm)
	Control H_2O	–	7	
1	A	42	6.5–7.5	<5
2	B	40	5–6	50–140
3	C	28	5–6	50–140
4	D	43	4–5	12–40
5	E	45	6.5–7.5	<5

2.4. *Characterisation study*

The surface morphology of each of the gray cast iron sample used for the corrosion test were further characterised using scanning electron microscope integrated with Energy Dispersive Spectroscopy (SEM/EDS VEGA3 TESCAN) to detect the phenomenon and the possibility of material behaviour as a result of its interaction with the ethanol environment.

2.5. *Microhardness test*

The sample surface was ground using 180, 400 and 600 grit size SiC carbide abrasives. They were later polished and rinsed in alcohol and allowed to dry. Vickers hardness tester was employed in determining the indentation of each sample. A force of 500 N and dwell time of 15 s was selected. The size of indentation was measured for each sample as left by the pyramid shaped indenter on the sample surface.

2.6. *Thermal gravimetric test*

A mass of 2.8350 g was ground to maximise the surface area of the sample so as to improve the resolution and a temperature of 30 °C/min was applied for all the sample to ensure reproducibility. Universal V4.5A TA Instruments was used for the thermal stability as well as the decomposition kinetics of gray cast iron.

3. Results and discussion

3.1. *Corrosion study: weight loss measurement*

The weight of each sample was measured at the end of each polarisation resistant test to understand the weight loss process as a result of the media. Fig. 2 presents the plot for the potentiodynamic weight loss. The average weight loss of each sample was measured using a weighing balance. The result revealed that the weight loss of gray cast iron samples in the media increases over time with sample E-45% alc. Vol. concentration showing aggressive weight loss of 0.0008 mg and sample C 0.0007 mg. Water which served as control test solution also showed a rapid weight loss of about 0.0007 mg. Cast iron sample (B) showed a reduced weight loss of 0.0002 g. The trend of weight loss for each sample is a function of exposure time as well as the concentration of the solution. Thus, sample E-45% showed more aggression of weight loss compared to sample C and B. However, with a minimal difference of 0.0001 mg with the control sample (water). Hence, the weight loss of sample in control medium (water) was rapid due to the fact that water contain fast ions, thus, the possibility of the gray cast iron sample losing part of its surface.

3.2. *Linear potentiodynamic study*

Potentiodynamic study showed that there was a reduction in both the anodic and cathodic reactions thereby causing reduction in corrosion density as it is obvious that they all tend towards the negative side (Fig. 3). Although, the ethanol blends are mixtures of additives (water) which actually made the solution a weak acid, but predominantly ethanoic. Thus, slow corrosion rate was observed based on the polarisation curve (Fig. 3). Additionally, the presence of water and oxygen could make the ethanol solution to exhibit an inhibition behaviour, thereby leading to wet corrosion. Moreover, there was discontinuity in the oxide film formation at the interface of the gray

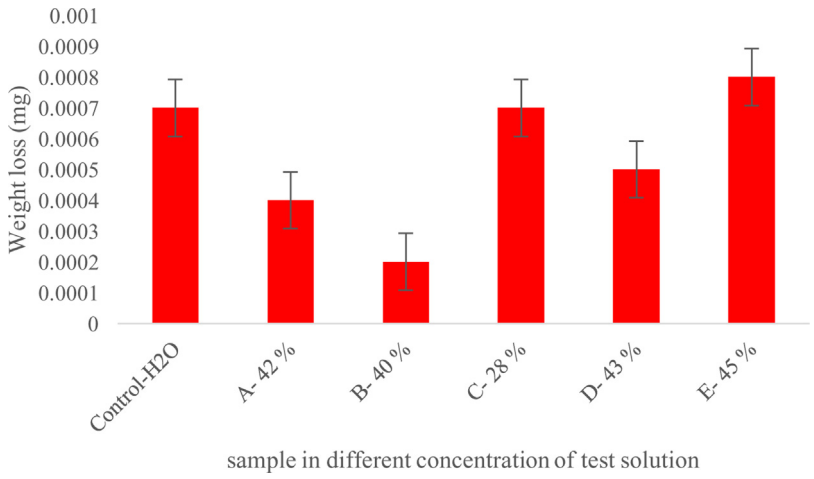

Fig. 2 – Potentiodynamic weight loss measurement for various samples.

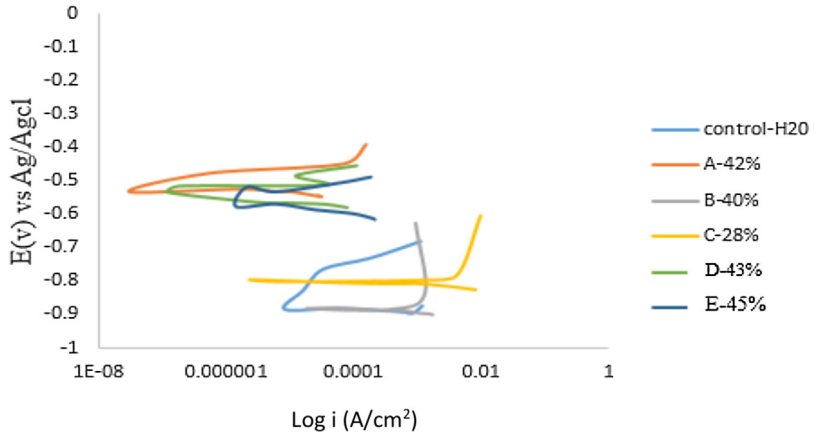

Fig. 3 – Potentiodynamic behaviour of different ethanol solutions on gray cast iron.

Table 3 – Polarisation study.

Sample ID	E_{Corr} (V)	I_{Corr} (A)	Polarisation resistance (R_P) (Ω)
A	−0.48574	−3.6271E−07	−7.1922
B	−0.87527	−2.2335E−06	
C	−0.79878	4.677E−05	
D	−0.58919	−4.4572E−07	
E	−0.48532	−2.1603E−07	
Control H_2O			

cast iron material which made it impossible for the metal to repassivate, and corrosion occurs slowly [23].

Further to this, from the tafel plots, all the ethanol samples could be observed to have their current density tending to the negative region compared to the control sample (water) which exhibited a slight current density on the positive mode. This is an indication that the ethanol samples exhibited an anti-corrosion behaviour [24].

The polarisation resistance result for each sample is presented in Table 3. It could be observed that there seems to be an excellent correlation between the polarisation resistance and the measured weight loss as seen for the sample A (Table 3). They both exhibited negative current density (Fig. 3 and Table 3). Although, the linear polarisation resistance measurement is instantaneous which made it more powerful, compared with the weight loss technique that depend on measured period in order to determine the corrosion rate. Thus, gray cast iron was observed to thrive well in such electrolyte.

3.3. *SEM/EDS studies*

Fig. 4 showed the microstructure of gray cast iron sample after the corrosion test in distilled water. It consists of graphite flakes and carbide layers at the metal interface but observed to be more concentrated at the boundaries. Compared with the surface morphology of as received gray cast iron (Fig. 1a), distilled water seems to have corroded the sample. Also, the EDS result showed that silicon was present (1.0%) thus, increasing the volume of graphite layers [25]. More so, chromium and manganese presence improved the hardness of the surface thereby increasing the wear and corrosion resistance of the distilled water [26].

Fig. 5 represent the surface morphology of the sample immersed in 42% alc. Vol. concentration of the test solution. It could be observed that oxide films were deposited at the surface of the metal. Also the oxide films formed on the cast iron

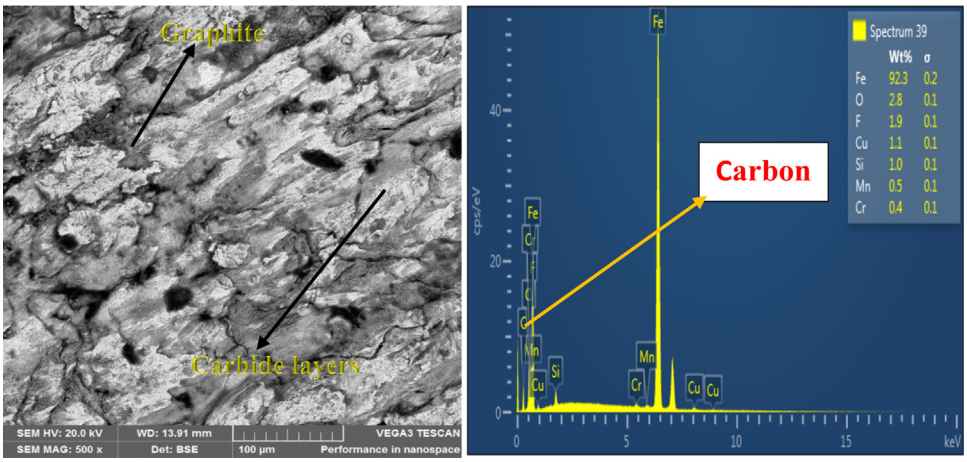

Fig. 4 – SEM/EDS of gray cast iron sample in H_2O (Control).

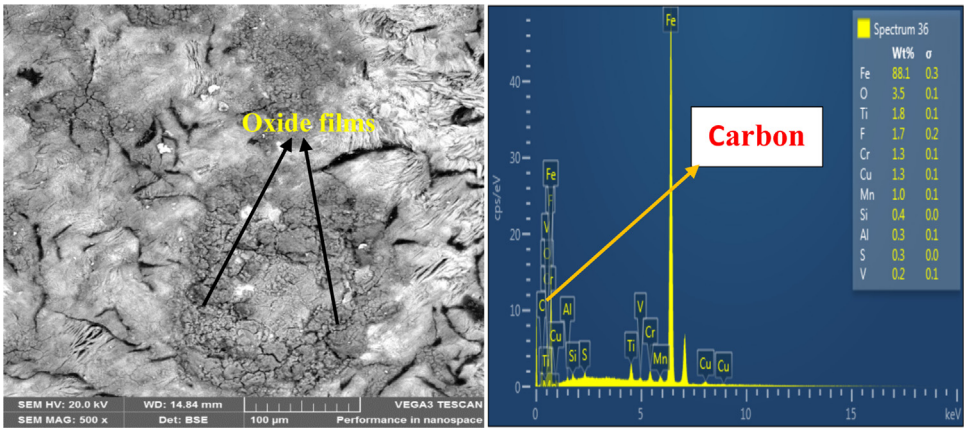

Fig. 5 – SEM/EDS of gray cast iron sample in (A) in 42% alc. Vol.

were observed to be uniform in thickness across the interface and they formed layers over one another. The oxide formed may be due to consistent reaction of the specimen with oxygen which is always desirable when the oxide is formed at room temperature because of its effectiveness in preventing corrosion attack. The EDS analysis revealed that the material is rich in iron, about (88.1% Fe). The presence of chromium enhanced the stability of the oxide film because of its high binding energy and it plays important function in the corrosion resistance as well as hardening mechanism of metals. Hong et al. [27] reported that Chromium, can be used to distribute oxide on alloys, thus it is worth saying that Cr element can be used to disperse and stabilise oxide on the metal surface.

Also Fig. 6 show the surface morphology of sample B in 40% test solution of ethanol beverage blend. Severe and localised cracks were observed at the interface. Also observed are white deposit which almost indicate the presence of chloride in the test solution. From the EDS result, the metal consists of oxide compound such as Fe, O, Cu, Mn, Si, Cr and S. Nickel has a little percentage of about 0.5 which is formed as a result of the penetration of the test solution at the interface. Thus, the contact between the oxide and the metal interface will result to corrosion defects which are observed on the surface.

Furthermore, Fig. 7 displayed the surface morphology and the EDS result of sample C subjected to corrosion test in 28% alc. vol. concentration. The entire surface was observed to be dominated with dark and white spot in the form of corrosion product. The findings from the EDS analysis showed that Fe, F, Si and O are the major element present. Silicon presence indicate iron carbide formation which might be the result of the white deposit observed at the interface.

The surface morphology and EDS result of sample D in 43% concentration of the test solution is presented on Fig. 8, whitish and thin oxide layers were observed. The EDS result also showed the presence of Fe, O, Si, Zn, Mn, Ca and Cr. The presence of iron prevents cracking of the surface, while oxygen reacts with silicon to form silicon oxides on the surface while manganese presence promotes pearlite formation. Fig. 9 presents the surface morphology of sample E of 45% concentration of the test solution. The microstructure is dominated by white corrosion product and evidence of groove at the interface with no severe surface damage at the interface. The EDS

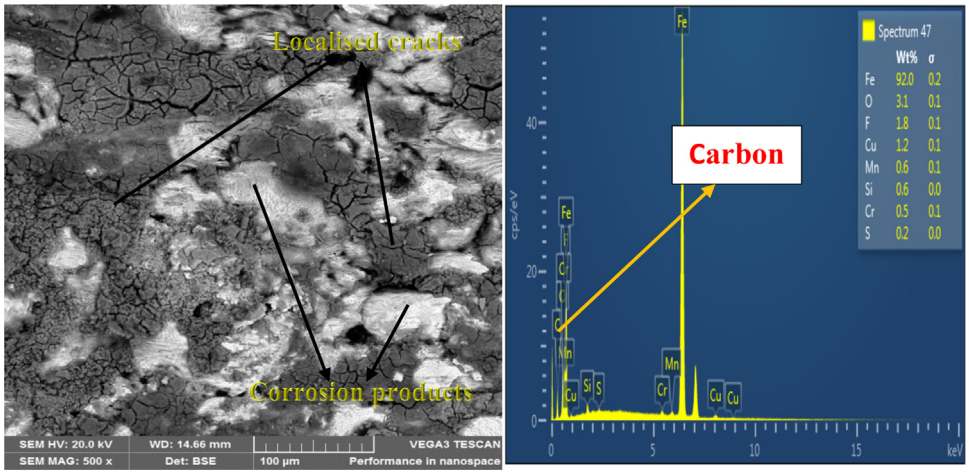

Fig. 6 – SEM/EDS of gray cast iron sample in (B) in 40% alc. Vol.

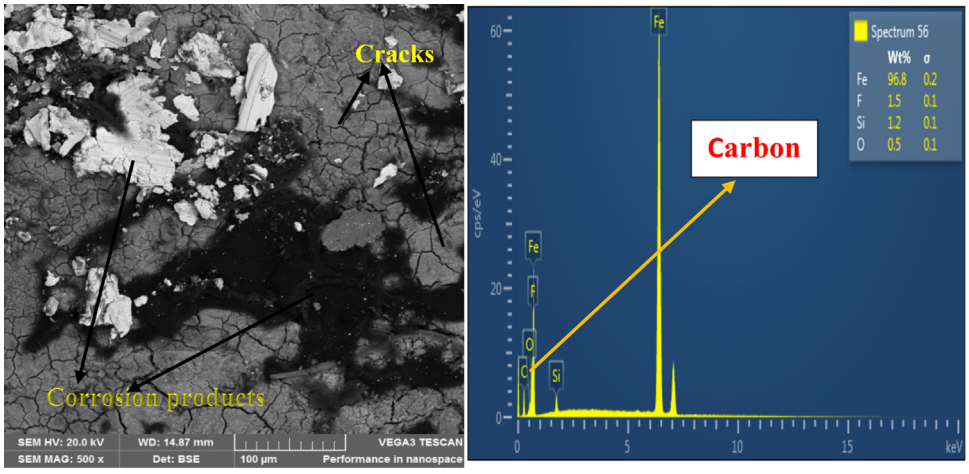

Fig. 7 – SEM/EDS of gray cast iron sample in (C) in 28% alc. Vol.

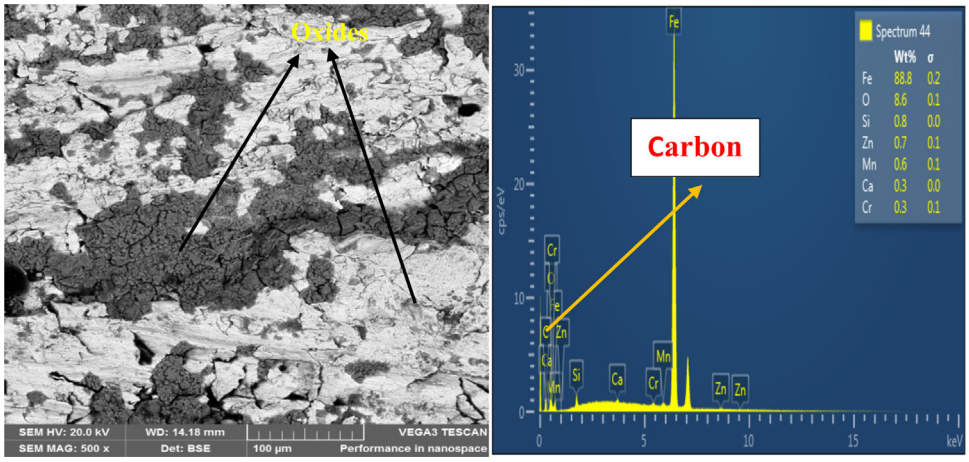

Fig. 8 – SEM/EDS of gray cast iron sample in (D) in 43% alc. Vol.

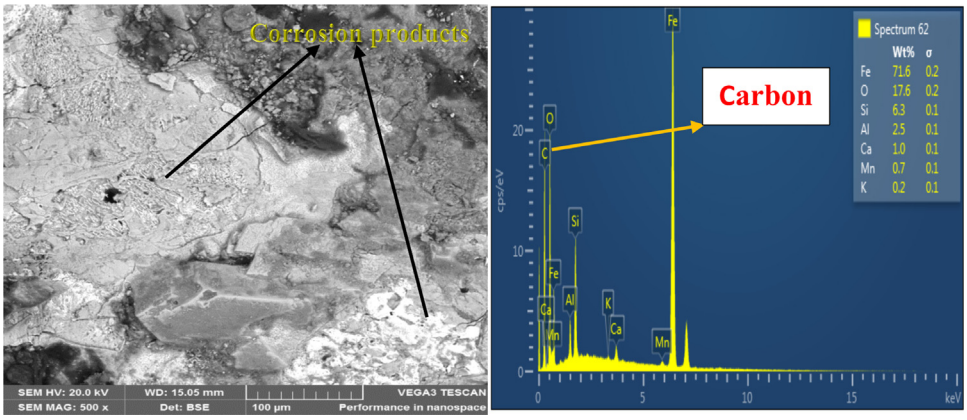

Fig. 9 – SEM/EDS of gray cast iron sample in (E) in 45% alc. Vol.

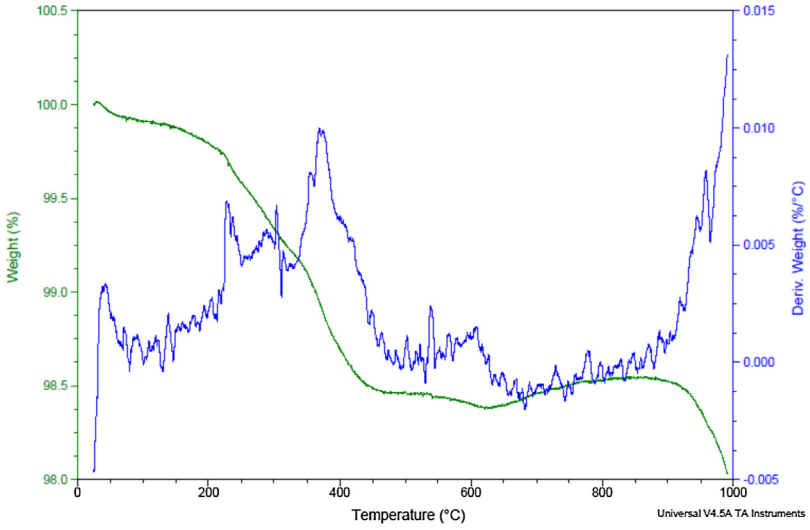

Fig. 10 – DSC-TGA curves of gray cast iron sample in distilled H_2O (Control).

result showed that the gray cast iron have high percentage of iron present and fractions of other component element.

3.4. *Thermal gravimetric analyses*

Stability analysis of the cast iron metals subjected to weight loss was carried out using thermal gravimetric analyser. Fig. 10 present the thermal gravimetric analysis of the control sample. In this case, the highest temperature was reached at 990 °C. This indicate that thermal stability can be determined at this point. The effect of heat flow on the sample mass loss was investigated using the same heating rate of 30 °C/min for all sample. It was clear that the peak temperature indicates the thermal degradation point for each sample. The findings from this work is in line with study by Zhang et al. [28] which reported that TGA is fundamentally used to measure the evolved mass loss of samples under temperature condition and atmosphere. Fig. 11 showed the thermal behaviour of 2.8350 mg of cast iron material subjected to initial heating at 30 °C/min. Gradual weight loss was observed from the starting temperature up to a temperature of 410 °C. Consequently, initial thermal decomposition started at the temperature 410 °C up to 995 °C. this indicate that there was weight loss of about 0.002 deriv. weight (%/°C) of the material. Hence, thermal degradation will ensue under real life application.

Fig. 12 showed sample B thermal behaviour which indicate that there was a rapid weight gain from a temperature of 30 °C/min up to 350 °C. Also, from this point the curve showed a decrease in the trend indicating that there was weight loss in the material. Thermal stability of the material was observed at 350 °C up to 990 °C. Consequently, with the initial starting temperature of 30 °C/min. Also, sample C (Fig. 13) showed a similar trend in weight loss. However, the thermal stability was observed at almost the final heating temperature which indicate that it took more time for it to decompose. Also, Figs. 14 and 15 showed similar trend in weight loss as both had

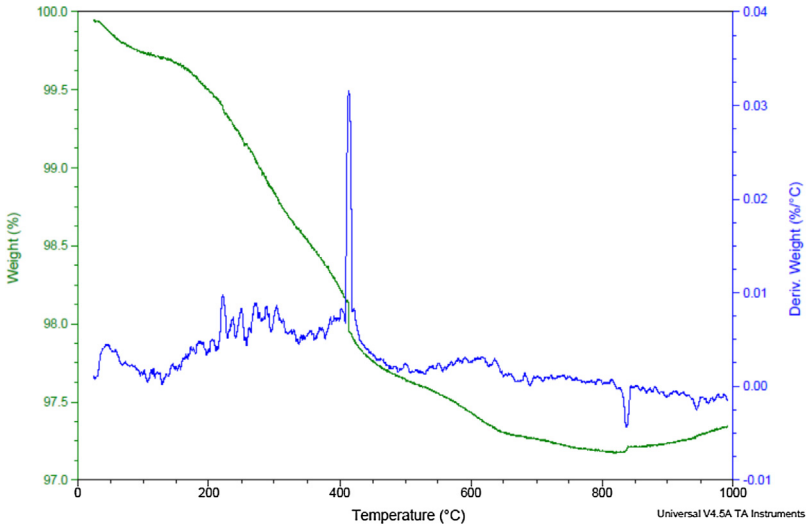

Fig. 11 – DSC–TGA curves of gray cast iron in sample (A) 42% alc. Vol. conc.

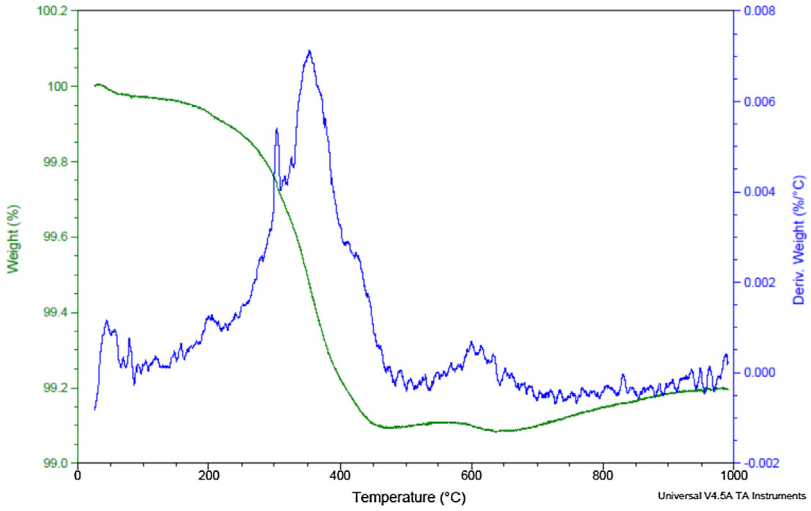

Fig. 12 – DSC–TGA curves of gray cast iron in sample (B) 40% alc. Vol. conc.

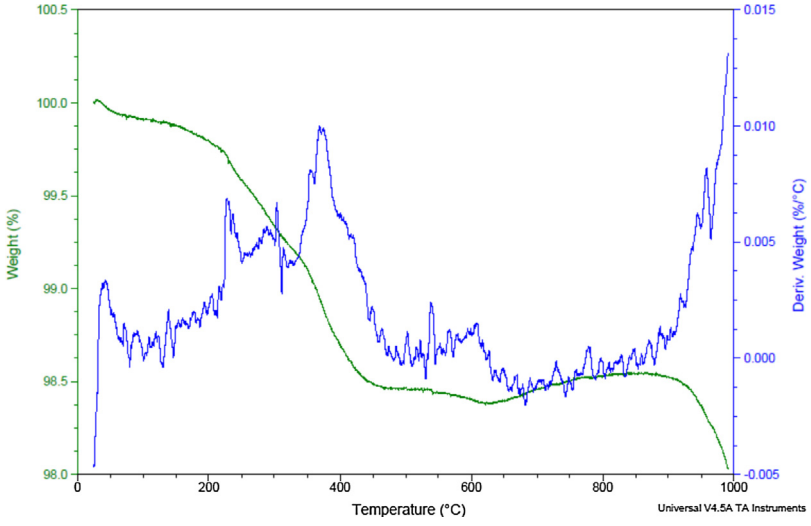

Fig. 13 – DSC–TGA curves of gray cast iron in sample (C) 28% alc. Vol. conc.

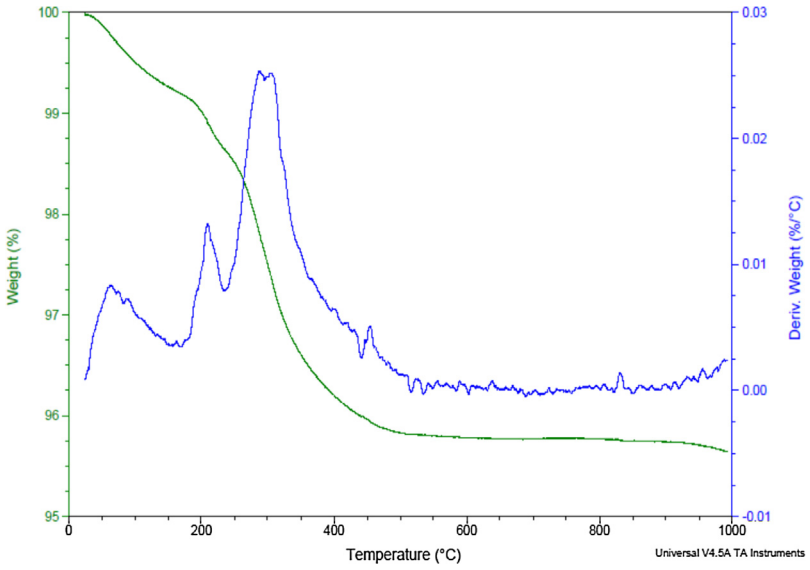

Fig. 14 – DSC–TGA curves of gray cast iron in sample (D) 43% alc. Vol. conc.

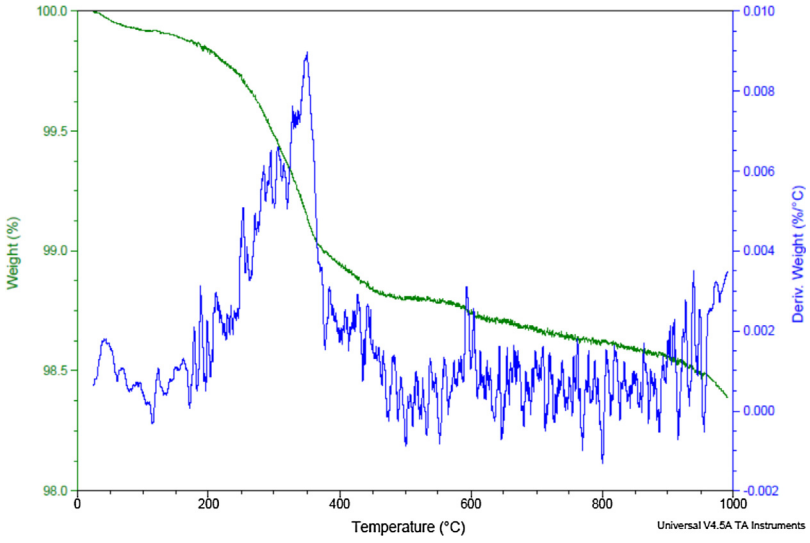

Fig. 15 – DSC–TGA curves of gray cast iron in sample (E) 45% alc. Vol. conc.

their thermal decomposition at 280 °C. However, there seems to be slight variation in the rate of weight loss which can be attributed to the initial sample size or mass.

Thus, in both cases, weight loss occurred due to thermal degradation. However, it is less in gray cast iron due to the presence of graphite which served as lubricant. Hence, gray cast iron material will function better under the application environment.

3.5. *Micro-hardness measurements of the gray cast iron samples after immersion test*

Fig. 16 showed the variation in hardness values of the gray cast iron material after the weight loss experiment. Due to carbon existence in the gray cast iron which is in the form of graphite, soft iron of reduced density was formed during the test. Also, the presence of sulphur in cast iron forms iron sulphide which increases the hardness. Thus, there was no much variation in the hardness values due to the aforementioned properties of cast iron in general. However, the micro-hardness of sample E reduced drastically to about 190.01 Hv compared to as-received material. This might be as a result of the additives present as well as the concentration of the test solution. Further to this, based on the result of the hardness behaviour of gray cast iron in the ethanol blend solution, it is worthy of note that gray cast iron showed good corrosion resistance. Thus, the gray cast iron material showed minimal reduction in hardness values in the ethanol solutions due to the presence of graphite and chromium.

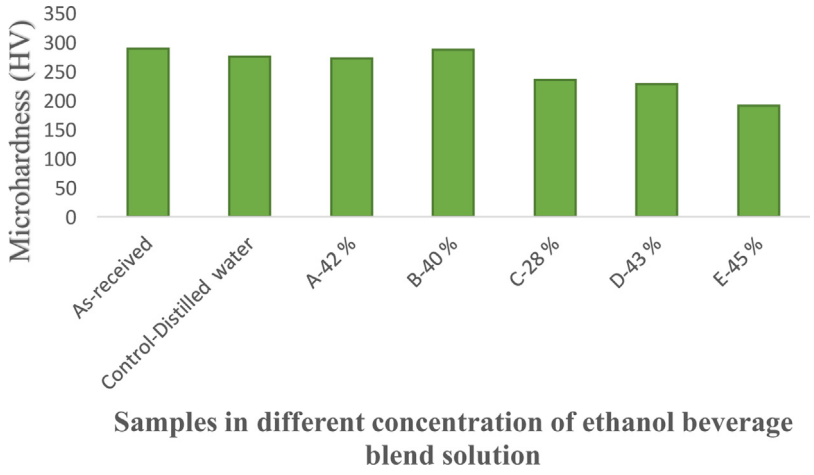

Fig. 16 – Plot of micro-hardness for gray cast iron samples immersed in different test solutions.

4. Conclusion

The result of the present study has demonstrated that, the behaviour of gray cast iron in varying concentrations of different ethanol blend varies due to different concentrations and additives. The effects on microstructure, weight loss and thermal gravimetric were investigated to determine the integrity of the cast iron material under environment of application. More so, the improvements on the corrosion rate by the ethanol media demonstrates their individual compositions and this suggests the possibility of employing gray cast iron materials in such application environment.

The microstructural evolutions showed that, the surface asperities formed adsorbents or reactive atoms to prevent oxygen and the test solutions from penetrating through. This is the reason behind the oxide formed at the surface of most of the microstructure. Further to this, the thin oxide films formed multilayers on the surface of the metal and subsequent corrosion protection. Also, stress induced fatigue which could have resulted to increased wear would be reduced.

The TGA analysis showed that various weight increase was due to surface oxide formed while weight loss occurs as a result of oxidising atmosphere. These findings guide in understanding the concept of thermal runaway in which temperature increase in the material causes the change in the behaviour of the structural compositions and subsequent destructive results such as thermal stress. Comparison of the micro-hardness result of the samples in the different test solutions with the as received showed minimal reduction in hardness value. This however, implies that, the gray cast iron will survive in the ethanol environment over a long period of time. Summing up, the electrochemical study and thermal gravimetric behaviour of gray cast iron in ethanol environment demonstrates the possibilities of controlling the process of material selection for gear applications in such environment.

Conflicts of interest

The authors declare no conflicts of interest.

Acknowledgement

The authors thank the management of Covenant University for supporting this project.

REFERENCES

[1] Zhou M, Liu H, Kang C, Wei X. Resistance of curved surfaces to the cavitation erosion produced through high-pressure submerged waterjet. Wear 2019:203091.
[2] Radi PA, Vieira A, Manfroi L, de Farias Nass KC, Ramos MAR, Leite P, et al. Tribocorrosion and corrosion behavior of stainless steel coated with DLC films in ethanol with different concentrations of water. Ceram Int 2019;45(7):9686–93.
[3] Tomić T, Milčić M, Nasipak NU, Babić S. Determination of chloride and sulfate in bio-ethanol by ion chromatography. Ind J Chem Technol 2016;23:65–70.
[4] Umoren SA, Solomon MM, Eduok UM, Obot IB, Israel AU. Inhibition of mild steel corrosion in H_2SO_4 solution by coconut coir dust extract obtained from different solvent systems and synergistic effect of iodide ions: ethanol and acetone extracts. J Environ Chem Eng 2014;2(2):1048–60.
[5] Dong Z, Zhou T, Liu J, Zhang X, Shen B, Hu W, et al. Cavitation erosion behaviors of surface chromizing layer on 316L stainless steel. Ultrason Sonochem 2019;58:104668.
[6] Okwuobi S, Ishola F, Ajayi O, Salawu E, Aworinde A, Olatunji O, et al. A reliability-centered maintenance study for an individual section-forming machine. Machines 2018;6(4):50.
[7] Salawu EY, Ajayi OO, Inegbenebor AO. Predictive modelling of a K-unit bottling plants for reliability improvement. Procedia Manuf 2019;35:91–6.
[8] Salawu EY, Ajayi OO, Inegbenebor AO, Afolalu SA. Constitutive model to analyse the effect of variation in temperature distribution on the rate of heat transfer around a spur gear tooth. Procedia Manuf 2019;35:236–41.
[9] Dalmau A, Richard C, Igual–Muñoz A. Degradation mechanisms in martensitic stainless steels: wear, corrosion and tribocorrosion appraisal. Tribol Int 2018;121:167–79.
[10] Sulaiman KO, Onawole AT, Faye O, Shuaib DT. Understanding the corrosion inhibition of mild steel by selected green compounds using chemical quantum based assessments

and molecular dynamics simulations. J Mol Liq 2019;279:342–50.
[11] Sin HLY, Rahim AA, Gan CY, Saad B, Salleh MI, Umeda M. *Aquilaria subintergra* leaves extracts as sustainable mild steel corrosion inhibitors in HCl. Measurement 2017;109:334–45.
[12] Fatoba OS, Aigbodion VS. Experimental study of hardness values and corrosion behaviour of laser alloyed Zn–Sn–Ti coatings of UNS G10150 mild steel. J Alloys Compd 2016;658:248–54.
[13] Sadeghi A, Moloodi A, Golestanipour M, Shahri MM. An investigation of abrasive wear and corrosion behavior of surface repair of gray cast iron by SMAW. J Mater Res Technol 2017;6(1):90–5.
[14] Salawu EY, Ajayi OO, Inegbenebor A, Akinlabi S, Akinlabi E. Influence of pulverized palm kernel and egg shell additives on the hardness, coefficient of friction and microstructure of gray cast iron material for advance applications. Results Eng 2019;3:100025.
[15] Neville A, Hodgkiess T, Xu H. An electrochemical and microstructural assessment of erosion–corrosion of cast iron. Wear 1999;233:523–34.
[16] Krishnamurthy N, Jain R. Corrosion kinetics of $Al_2O_3 + ZrO_2{\cdot}5CaO$ coatings applied on gray cast iron substrate. Ceram Int 2017;43(17):15708–13.
[17] Al-Shama LM, Saleh JM, Hikmat NA. Potentiostatic studies of the corrosion of gray cast iron in sulphuric acid and sodium hydroxide solutions. Corros Sci 1987;27(3):221–8.
[18] Zulhishamuddin AR, Aqida SN, Rashidi MM. A comparative study on wear behaviour of Cr/Mo surface modified gray cast iron. Opt Laser Technol 2018;104:164–9.
[19] Zhou YX, Zhang J, Xing ZG, Wang HD, Lv ZL. Microstructure and properties of NiCrBSi coating by plasma cladding on gray cast iron. Surf Coat Technol 2019;361:270–9.
[20] Zhao N, Zhao Y, Li J, Wang X, Wei Y, Tang K, et al. Formation mechanism and single abrasive wear of TaC dense ceramic layer on surface of gray cast iron. Ceram Int 2019;45(12):15580–8.
[21] Medyński D, Janus A. Effect of heat treatment parameters on abrasive wear and corrosion resistance of austenitic nodular cast iron Ni–Mn–Cu. Arch Civil Mech Eng 2018;18(2):515–21.
[22] Zhu L, Liu Y, Li Z, Zhou L, Li Y, Xiong A. Microstructure and properties of Cu–Ti–Ni composite coatings on gray cast iron fabricated by laser cladding. Opt Laser Technol 2020;122:105879.
[23] Proverbio E, Calabrese L, Caprì A, Bonaccorsi L, Dawoud B, Frazzica A. Susceptibility to corrosion of aluminium alloy components in ethanol adsorption chiller. Renewable Energy 2017;110:174–9.
[24] Salawu EY, Ajayi OO, Inegbenebor A, Fayomi OSI, Uyor UO. Corrosion behavior of mild steel in different concentrations of ethanol beverages. J Bio Tribo Corros 2020;6(1):2.
[25] Agunsoye JO, Isaac TS, Awe OI, Onwuegbuzie AT. Effect of silicon additions on the wear properties of gray cast iron. J Miner Mater Character Eng 2013;1(02):61.
[26] ELSawy EET, EL-Hebeary MR, El Mahallawi ISE. Effect of manganese, silicon and chromium additions on microstructure and wear characteristics of gray cast iron for sugar industries applications. Wear 2017;390:113–24.
[27] Hong KH, Kim JH, Chang K, Kwon J. The role of Cr on oxide formation in Ni-Cr alloys: a theoretical study. Comput Mater Sci 2018;142:185–91.
[28] Zhang T, Wang Z, Wang Y, Wei Z, Li X, Hou X, et al. The characteristics of free/bound biomarkers released from source rock shown by stepwise Py-GC-MS and thermogravimetric analysis (TGA/DTG). J Petrol Sci Eng 2019.